Accepted Manuscript

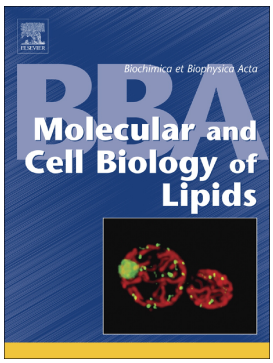

Phospholipase D1 downregulation by α-synuclein: Implications for neurodegeneration in Parkinson's disease

Melisa A. Conde, Natalia P. Alza, Pablo Iglesias Gonzalez, Paola G. Scodelaro Bilbao, Sofia Sánchez Campos, Romina M. Uranga, Gabriela A. Salvador

PII: S1388-1981(18)30047-7
DOI: doi:10.1016/j.bbalip.2018.03.006
Reference: BBAMCB 58262

To appear in:

Received date: 6 September 2017
Revised date: 14 March 2018
Accepted date: 18 March 2018

Please cite this article as: Melisa A. Conde, Natalia P. Alza, Pablo Iglesias Gonzalez, Paola G. Scodelaro Bilbao, Sofia Sánchez Campos, Romina M. Uranga, Gabriela A. Salvador , Phospholipase D1 downregulation by α-synuclein: Implications for neurodegeneration in Parkinson's disease. The address for the corresponding author was captured as affiliation for all authors. Please check if appropriate. Bbamcb(2018), doi:10.1016/j.bbalip.2018.03.006

Phospholipase D1 downregulation by α-synuclein: implications for neurodegeneration in Parkinson's disease.

Melisa A. Conde[a,b,d,+], Natalia P. Alza[a,c,d,+], Pablo Iglesias Gonzalez[a,d], Paola G. Scodelaro Bilbao[b,d], Sofia Sánchez Campos[b], Romina M. Uranga[a,b,d], Gabriela A. Salvador[a,b,d,*]

[a] *Instituto de Investigaciones Bioquímicas de Bahía Blanca (INIBIBB)*

[b] *Departamento de Biología, Bioquímica y Farmacia-Universidad Nacional del Sur (UNS)*

[c] *Departamento de Química-UNS*

[d] *Consejo Nacional de Investigaciones Científicas y Técnicas (CONICET), Bahía Blanca, Argentina*

***Corresponding author:** Gabriela A. Salvador, Instituto de Investigaciones Bioquímicas de Bahía Blanca, La Carrindanga Km 7, 8000 Bahía Blanca, Buenos Aires, Argentina. Tel.: +54-291-4861201. Fax: +54-291-4861200. E-mail: salvador@criba.edu.ar.

+ These authors contributed equally to this work.

Abstract

We have previously shown that phospholipase D (PLD) pathways have a role in neuronal degeneration; in particular, we found that PLD activation is associated with synaptic injury induced by oxidative stress. In the present study, we investigated the effect of α-synuclein (α-syn) overexpression on PLD signaling. Wild Type (WT) α-syn was found to trigger the inhibition of PLD1 expression as well as a decrease in ERK1/2 phosphorylation and expression levels. Moreover, ERK1/2 subcellular localization was shown to be modulated by WT α-syn in a PLD1-dependent manner. Indeed, PLD1 inhibition was found to alter the neurofilament network and F-actin distribution regardless of the presence of WT α-syn. In line with this, neuroblastoma cells expressing WT α-syn exhibited a degenerative-like phenotype characterized by a marked reduction in neurofilament light subunit (NFL) expression and the rearrangement of the F-actin organization, compared with either the untransfected or the empty vector-transfected cells. The gain of function of PLD1 through the overexpression of its active form had the effect of restoring NFL expression in WT α-syn neurons. Taken together, our findings reveal an unforeseen role for α-syn in PLD regulation: PLD1 downregulation may constitute an early mechanism in the initial stages of WT α-syn-triggered neurodegeneration.

Keywords

Phospholipase D1, α-synuclein, Neurofilament, Phosphatidic acid, Neurodegeneration, Parkinson's disease.

Abbreviations

α-syn, alpha synuclein; AU, arbitrary units; CF, cytosolic fraction; DAG, diacylglycerol; ERK, extracellular signal-regulated kinase; ev, IMR-32 cell line stably transfected with pcDNA empty vector; IMR32, human neuroblastoma cell line; LW, Lewy bodies; MAPKs, mitogen-activated protein kinases; MEK, MAPK kinase; NF, nuclear fraction; NFH, neurofilament heavy subunit; NFL, neurofilament light subunit; NFM, neurofilament medium subunit; PA, phosphatidic acid; PD, Parkinson's disease; PEth, phosphatidylethanol; PKC, protein kinase C; PLD, phospholipase D; PLD1i, specific pharmacological PLD1 inhibitor; PLD2i, specific pharmacological PLD2 inhibitor; qRT-PCR, quantitative real-time polymerase chain reaction, ut, IMR-32 untransfected cells; WT, wild type; WT α-syn, IMR-32 cell line overexpressing human wild type α-syn.

1. Introduction

Phospholipase D (PLD) catalyzes the hydrolysis of head groups from phospholipids in order to produce phosphatidic acid (PA). PA is a lipid messenger that participates in multiple signaling processes involved in cell proliferation, membrane trafficking, hormone response and cytoskeletal organization, among others [1–3]. PLD1 and PLD2 isoforms have been described and extensively characterized in most cell types and tissues. Both isozymes are specific for cleaving phosphatidylcholine and are differentially regulated mainly because they possess distinct cellular localization and functions [4].

In neurons, PLD1 has been shown to regulate cytoskeleton architecture and is thus involved in dendritic branching and spine regulation, contributing to neuronal development [5,6]. PA produced by PLDs and by the phosphorylation of diacylglycerol (DAG) by DAG kinases has also been described as a key regulator of synaptic vesicle trafficking and neurotransmission [7]. Considering these key elements in proper neuronal function, it is highly likely that impairment of PLD signaling leads to neuronal degeneration. Indeed, it has been reported that PLD signaling failures are present in Alzheimer's disease and, as a result, this lipid pathway has been proposed as an emerging therapeutic target [1]. On the contrary, the role of PLDs in Parkinson's disease (PD), the second most common neurodegenerative disorder in the elderly, has not been completely elucidated.

PD is characterized by the progressive death of dopaminergic neurons in the *substantia nigra pars compacta* and the presence of the cytosolic inclusions called Lewy bodies (LB). LB's main component is the misfolded protein α-synuclein (α-syn) [8] which is very abundant in neurons. Missense mutations or multiplication of α-syn-encoding gene are responsible for the early onset familial form of PD [9]. Despite efforts to arrive at a

better understanding of the physiological and pathological implications of α-syn, the mechanisms involved in its toxicity remain unclear. An intriguing and still not fully characterized property of α-syn is its involvement in cell lipid physiology. This presynaptic protein has been shown to present high binding affinity for fatty acids, cholesterol and phospholipids [10]. It has also been reported that α-syn not only binds and interacts with several lipid moieties but also modulates the activity of lipid metabolizing enzymes, such as acyl-CoA synthase, and the fatty acid uptake in astrocytes [11–13]. However, there is a divergence of findings on the molecular mechanisms operating between α-syn and PLD. Whereas *in vivo* experiments have demonstrated that α-syn is able to hinder PLD2 activity [14], *in vitro* assays show no inhibitory properties of α-syn on PLD activities [15]. More recently, it has been reported that the pharmacological inhibition of PLD1 interferes with the autophagic flux and triggers the accumulation of aggregated α-syn [16]. In the same study, it was reported that *post mortem* brains obtained from LB dementia patients display diminished PLD1 expression [16].

Regarding the role of PLD in neurodegeneration, we have previously demonstrated that PLD signaling is activated in the synaptic response to oxidative stress and inflammation [17–19]. Studies performed in transgenic mice have demonstrated that genetic deletion of PLD1 or PLD2 delays brain development and also alters cognitive function in adults [20]. However, the role of PLD deletion in PD pathology has not been clearly elucidated in animal models [21]. In the current study, we investigated the status of the PLD1 pathway in human neuroblastoma cells (IMR-32) overexpressing human wild-type α-syn (WT α-syn). For this purpose, we worked with three cellular models: untransfected (ut) IMR-32 cells, and cells stably transfected with either WT α-syn or the empty pcDNA vector (ev). Our results show that WT α-syn is able to inhibit PLD1

expression and to alter ERK1/2 signaling. Both events are related to a decrease in neurofilament light chain (NFL) and to altered actin cytoskeleton. Interestingly, restoration of PLD1 expression promotes NFL recovery. Our results suggest that PLD1 inhibition induced by WT α-syn triggers neuronal cytoskeleton alterations during the early stages of the neurodegeneration process.

2. Materials and methods

2.1. Materials

Antibodies: rabbit polyclonal anti-α-synuclein (C-20-R) (catalog no. sc-7011-R), rabbit polyclonal anti-ERK2 (catalog no. sc-154), mouse monoclonal anti-β-actin (catalog no. sc-47778), mouse monoclonal IgG_{2A} hnRNP (catalog no. sc-32301), polyclonal horseradish peroxidase (HRP)-conjugated mouse anti-rabbit IgG (catalog no. sc-2357), HRP-conjugated m-IgGκ (catalog no. sc-516102) and normal anti-mouse IgG_{2A} (catalog no. sc-3878) were purchased from Santa Cruz Biotechnology, Inc. (Santa Cruz, CA, USA). Rabbit polyclonal anti-α-synuclein (catalog no. cs-2642S), rabbit polyclonal anti-PLD1 (catalog no. cs-3832S), rabbit polyclonal anti-p-P44/42 MAPK (T202/Y204) (catalog no. cs-9101S), and rabbit polyclonal anti-P44/42 MAPK (catalog no. cs-9102S) were purchased from Cell Signaling Technology (Beverly, MA, USA). Mouse monoclonal anti-neurofilament clone DA2 (catalog no. mab1615) was purchased from Millipore (Bedford, MA, USA). Mouse monoclonal anti-α-tubulin (catalog no. CP06) was purchased from Calbiochem (Sigma Aldrich Co., St. Louis, MO, USA).

Alexa Fluor 488 goat anti-mouse (catalog no. A-11001) and Alexa Fluor 546 goat anti-rabbit (catalog no. A-11035) were purchased from Thermo Fisher (Invitrogen, CABA, Bs. As., Argentina). Alexa Fluor 405 goat anti-mouse (catalog no. ab175658) was obtained from Abcam (Tecnolab, Bs. As., Argentina). Cy-2-conjugated goat anti-rabbit

(catalog no. 111-225-144) was obtained from Jackson Immunoresearch (Sero-immuno Diagnostics, GA, USA).

Rhodamine phalloidin (catalog no. R415), TO-PRO®-3 iodide (642/661) (catalog no. T-3605) and Hoechst (catalog no. C-10339) were purchased from Thermo Fisher (Invitrogen, CABA, Bs. As., Argentina). Polyvinylidene difluoride (PVDF) membranes were purchased from EMD Millipore (Millipore, Bedford, MA, USA). DMEM medium, trypsin and antibiotic-antimycotic were obtained from Gibco (USA). Geneticin (G418), VU0155069, CAY10594and U0126 were purchased from Santa Cruz Biotechnology, Inc. (Santa Cruz, CA, USA). Fetal bovine serum (FBS) was obtained from Natocor (Córdoba, Argentina). 3-(4,5-dimethylthiazol-2-yl)-2,5 diphenyltetrazolium bromide (MTT) was obtained from Sigma-Aldrich (St. Louis, MO, USA). Lipofectamine 2000 was purchased from Invitrogen. Radiolabeled oleic acid [9,10-^{3}H(*N*)] ([^{3}H]-OA) (15–60 Ci/mmol) was purchased from New England Nuclear-Dupont (Boston, MA, USA.) All other chemicals used in the present study were of the highest purity available.

2.2. Cell culture and stable expression of wild-type α-synuclein

The immortalized human neuroblastoma cell line IMR-32 was obtained from ATCC. Cells were grown in DMEM-high glucose medium supplemented with 10% (v/v) FBS, 100 U/mL penicillin, 100 µg/mL streptomycin and 0.25 µg/mL amphotericin B in a humidified atmosphere of 5% CO_2 at 37°C.

The expression vector containing the native form of the human α-synuclein sequence, pcDNA3-WT-α-syn, was kindly donated by Dr. B. Wolozin. Both pcDNA3-WT-α-syn and pcDNA3 vectors were transfected into IMR-32 cells using Lipofectamine 2000 reagent following the procedure recommended by the manufacturer. The stable transfected cells were selected 72 h post-transfection in the presence of 400 µg/ml of geneticin (G418) and further maintained in DMEM high glucose growth medium

supplemented with 200 µg/ml G418. Expression levels of α-syn were confirmed by dot blot, Western blot and immunocytochemistry. Expression plasmids eGFP-PLD1 and HA-ERK2 were kindly donated by Dr. M. Frohman and Dr. S. Gutking, respectively.

2.3. Experimental treatments

Cells were grown to 80-90% confluence and all treatments were carried out in serum-free medium. Treatments with inhibitors were performed as follows: medium was removed and replaced with serum-free medium. Inhibitors were subsequently added to the desired final concentration [5 µM PLD1i and PLD2i, 10 µM MEK 1/2 inhibitor, controls received vehicle alone (0.05% dimethyl sulfoxide (DMSO)] and cells were incubated under these conditions for 24 h unless otherwise specified [18].

2.4. Immunofluorescence microscopy

IMR-32 cells stably expressing WT α-syn, the empty vector (ev) or non-transfected (ut) cells were grown onto glass coverslips and the growing medium was replaced by serum-free medium. After treatment for 24 h, cells were fixed for 20 min with 4% paraformaldehyde in PBS. For the immunostaining, cells were permeabilized and the non-specific sites were blocked with 2% bovine serum albumin (BSA) in PBS and Triton X-100 (0,1%) at room temperature for 45 min. Cells were incubated with the appropriate primary antibody (1:100 in PBS, 2% BSA, 0,1% Triton X-100; 1 h at room temperature). After three washes with PBS, cells were incubated with the appropriate fluorescent secondary antibody (1:300; 1 h at room temperature) and Hoechst or TO-PRO®-3 for nuclear staining. For F-actin staining, cells were incubated with rhodamine phalloidin after nuclear staining (1:200 in PBS; 30 min at room temperature). After washing with PBS, coverslips were mounted, and slides were observed with a Nikon Eclipse E-600 microscope. Quantification was performed using ImageJ (a freely

available application in the public domain for image analysis and processing, developed and maintained by Wayne Rasband at the Research Services Branch, National Institute of Health, Bethesda, MD, USA) and at least 100 cells for each condition were analyzed from two independent cell cultures.

2.5. Assessment of cell viability

Briefly, cells (5 x 10^4 cells/well) were incubated for 24 h in serum-free medium and cell viability was determined by MTT reduction assay. Viable cells reduced MTT to a colored, water insoluble formazan salt. After treatment, MTT (5 mg/ml) was added to the cell culture medium at a final concentration of 0.5 mg/ml. After incubating the plates for 2 h at 37ºC in a 5% CO_2 atmosphere, the assay was stopped and the MTT-containing medium was replaced with solubilization buffer (20% SDS, pH 4.7). The extent of MTT reduction was measured spectrophotometrically at 570 nm [22]. Results are expressed as a percentage of the control or arbitrary units.

2.6. Western blot analysis

For the preparation of total cell extracts, cells (1×10^7 cells) were rinsed with PBS, scraped and centrifuged. The pellet was rinsed with PBS and resuspended in 80 µl of a buffer containing 50 mM Tris pH 7.5, 150 mM NaCl, 0.1% Triton X-100, 1% NP-40, 2 mM EDTA, 2 mM EGTA, 50 mM NaF, 2 mM β-glycerophosphate, 1 mM Na_3VO_4, 10 µg/ml leupeptin, 5 µg/ml aprotinin, 1 µg/ml pepstatin, 0.5 mM PMSF, and 0.5 mM DTT. Samples were exposed to one cycle of freezing and thawing, incubated at 4°C for 60 min and centrifuged at 10000 x *g* for 20 min. The supernatant was decanted, and the protein concentration was measured according to Bradford [23]. Cell lysates containing 25–50 µg of protein were separated by reducing 7–12.5% polyacrylamide gel electrophoresis (PAGE) and electroblotted onto PVDF membranes. Molecular weight

standards (Spectra™ Multicolor Broad Range Protein Ladder, Thermo Scientific) were run simultaneously [24]. Membranes were blocked with 5% nonfat dry milk in TBS-T buffer for 1 h at room temperature and subsequently incubated overnight at 4ºC with primary antibodies (anti-α-syn, anti-PLD1, anti-p-P42/44 MAPK, anti-P42/44 MAPK and anti-NF clone DA2), washed three times with TBS-T and then exposed to the appropriate HRP-conjugated secondary antibody for 1 h at room temperature. Membranes were again washed three times with TBS-T and immunoreactive bands were detected by enhanced chemiluminescence using standard X-ray film. Immunoreactive bands were quantified using ImageJ.

2.7. Native PAGE electrophoresis

Cell lysates were prepared in a non-reducing non-denaturing sample buffer (62.5 mM Tris-HCl pH 6.8, 25% glycerol, 1% bromophenol blue) to maintain the secondary structure and native charge density of the proteins, separated in native PAGE and electroblotted onto PVDF membranes [25]. Membranes were fixed with 0.4% paraformaldehyde for 30 min at room temperature, rinsed with distilled water, blocked for 1 h at room temperature, and subsequently incubated for 1 h at room temperature with the primary antibody anti-α-syn, washed three times with TBS-T and then exposed to the appropriate HRP-conjugated secondary antibody for 1 h at room temperature. Membranes were washed three times with TBS and immunoreactive bands were detected by enhanced chemiluminescence using standard X-ray film.

2.8. Cytoplasmic and nuclear fractionation with NP-40-containing buffer

Nuclear and cytosolic fractions were isolated as described previously [26].

2.9. Quantitative reverse transcription-polymerase chain reaction (qRT-PCR)

Total RNA was isolated from IMR-32 ev and α-syn cells using TRIZOL Reagent (Invitrogen) according to the manufacturer's instructions. RNA was resuspended in nuclease-free water and its concentration was assessed from A260:A280 absorbance ratio in a PicoDrop Spectrophotometer. Samples were stored at −80°C until use. Aliquots containing 2 μg total RNA were used to synthesize cDNA in reactions containing 1 μg Random Primer hexamers (Biodynamics), 1X M-MLV Reverse Transcriptase Reaction Buffer, 0.5 mM of each dNTP, 25 UI RNase inhibitor (Promega) and 200 UI M-MLV Reverse Transcriptase (Promega). Reactants were taken to a final volume of 25 μl with RNase-free water [22].

The cDNA resulting from RT was amplified by real-time quantitative PCR. Gene expression levels were determined using Rotor-Gene 6000 (Corbett Research, Australia). qRT-PCR was performed in a final volume of 15 μl using Real Mix for Real-Time PCR (Bioline) and 0.4 μM of each primer. Gene-specific primers sequences were to PLD1, forward: CGTCCAGTGAGTCTGAGCAA and reverse: ATCTGGTTTCCCCATGCAGC and to RiboL32, forward: TGGAAGTGCTGCTGATGTGC and reverse: CACGATGGCTTTGCGGTTCT (purchased from Life Technologies). PCR conditions were as follows: 50 cycles of denaturation at 94°C for 20 s, annealing and extension at 58°C for 30 s and a final extension step at 72°C for 30 s. Ct values of PLD1 mRNA obtained from 3 different experiments were normalized according to the $2^{-\Delta Ct}$ method, using RiboL32 protein as a reference gene. At the end of the amplification phase, a melting curve analysis was carried out on the product formed and agarose gel electrophoresis was carried out to confirm product size. The relative level of PLD1 is expressed as the relative change in gene expression.

2.10. PLD activity assay

Confluent 60 mm dishes were treated for 24 h in serum-free DMEM with PLD1i, PLD2i, or vehicle and then were incubated for 24 h at 37°C with serum-free DMEM containing: [^{3}H]-OA (0.5 μCi/dish), oleic acid (1.5 μM) and lipid-free bovine serum albumin (4 mol oleic acid/mol BSA) to allow [^{3}H]-OA incorporation. After 24 h the medium was removed and serum-free DMEM with ethanol (2% vol/vol) was added. After 3 h the medium was removed, cells were washed three times with PBS, scraped off with 800 μl PBS, lipids were extracted and radiolabeled PEth, a PLD activity marker, was separated by one-dimensional thin-layer chromatography on silica gel H and developed with chloroform/methanol/acetone/acetic acid/water (50:15:15:10:5, vol/vol) up to 70% of the plate. To separate neutral lipids the TLC plate was rechromatographed up to the top using hexane/diethylether (70:30, vol/vol) [27]. PEth was visualized by exposure of chromatograms to iodine vapors, and then scraped off the plate into vials. Radioactivity corresponding to PEth was determined in a liquid scintillation spectrometer after the addition of 0.2 ml of water and 5 ml of 4% Omnifluor in toluene/Triton X-100 (t-octylphenoxypoly ethoxyethanol, 4:1, vol/vol) [28]. Lipid phosphorus was determined according to the method of Rouser et al. [29].

2.11. Statistical analysis

Data represent the mean value ± SD of at least three independent experiments. Statistical significance was determined by either Student's t-test or one-way ANOVA followed by a Tukey's test. *p*-values lower than 0.05 were considered statistically significant; *, ** or *** represent $p< 0.05$, $p< 0.01$ and $p< 0.001$ respectively.

3. Results

3.1. Characterization of WT α-syn-overexpressing IMR-32 neurons

We first characterized IMR-32 neurons stably transfected with pcDNA vector containing human WT α-syn. The expression of α-syn was investigated by using

different electrophoretic and blotting strategies for protein separation and detection. Increased levels of α-syn protein (200% increase) were observed in WT α-syn cells when compared with controls (cells transfected with the empty pcDNA vector, ev). The presence of α-syn monomers (19 kDa) and high molecular weight oligomers obtained from SDS-PAGE and non-denaturing gels, respectively, was also evident in WT α-syn cells (Fig. 1a).

It has been previously reported that *substantia nigra* samples from PD patients show reduced cellular content of neurofilament proteins [30]. Therefore, we investigated the expression of NFL in neurons overexpressing α-syn. WT α-syn neurons showed a strong decrease in NFL content when compared with control and ut cells (Fig. 1b). In addition, Sousa *et al.* demonstrated that α-syn overexpression is also able to alter actin cytoskeleton [31]. To examine the cytoskeleton architecture, we used phalloidin in order to detect F-actin arrangements. Whereas ut and control cells displayed a quite ordered F-actin arrangement, WT α-syn neurons showed the presence of actin-enriched loci in the cellular surface with no significant differences in total actin expression levels (Fig. 1c, white arrows). To further characterize the effect of WT α-syn overexpression, we checked neuronal viability by the MTT reduction assay. WT α-syn neurons showed a 20% decrease in cell viability compared to controls (Fig. 1d). These results associated with the 2-3-fold increase observed in α-syn expression led us to establish a cellular model of middle injury, that could mimic the first stages of PD-related neurodegeneration.

3.2. WT α-syn inhibits PLD1 expression

The role of α-syn in PLD activities has been a matter of debate [14,15,32]. More recently it has been demonstrated that PLD1 expression is decreased in brains from LB dementia patients where α-syn overexpression is a hallmark [16]. To examine the effect

of α-syn on PLD1, we first checked its levels of expression by Western blot. WT α-syn neurons exhibited decreased levels of PLD1 expression (70% decrease) when compared with controls (Fig. 2a). Consistently, mRNA levels determined by qRT-PCR were diminished (85% decrease) in WT α-syn neurons compared with controls (Fig. 2b). Immunocytochemistry studies displayed higher levels of PLD1 expression in ut cells and controls compared to WT α-syn cells (Fig. 2c). In all the tested experimental conditions PLD1 showed a predominant nuclear localization.

3.3. WT α-syn interferes with ERK1/2 pathway

Other authors have previously demonstrated that the overexpression of α-syn is able to alter MAPK pathways [33]. Taking this into account our next step was to evaluate the status of ERK1/2 phosphorylation and expression levels. We observed that not only ERK1/2 phosphorylation but also ERK2 expression were diminished (30% decrease) in WT α-syn neurons (Fig. 3a). By using immunocytochemistry, we also detected a differential ERK2 subcellular distribution: whereas ut and control cells displayed cytosolic ERK2 localization, the overexpression of WT α-syn induced ERK2 nuclear translocation (Fig. 3b). This fact was confirmed by subcellular fractionation experiments followed by immunoblotting: ERK1/2 content in the nuclear fraction (NF) of WT α-syn neurons showed to be increased (Fig. 3c). The purity of NF and cytosolic fraction (CF) was determined by testing the expression of the heterogeneous nuclear ribonucleoproteins (hnRNP, nuclear marker) and α-tubulin (cytosolic marker), respectively. The ratio nuclear/cytosolic ERK1/2 content was increased by 180% in WT α-syn cells, thus demonstrating that α-syn overexpression induced ERK1/2 nuclear confinement (Fig. 3c).

3.4. WT α-syn modulates PLD1/ERK1/2 signaling

We have previously demonstrated that ERK1/2 activation is regulated at least in part by PLD1 in several experimental models of cellular and synaptic injury [18,19]. To further validate the role of PLD1 in ERK1/2 regulation under α-syn-induced neuronal injury, we used the specific pharmacological PLD1 inhibitor (PLD1i), VU0155069. First, we checked the effect of PLD1 inhibition in ut cells. The basal state of ERK1/2 phosphorylation in IMR-32 ut neurons was inhibited (30% decrease) by the presence of PLD1i (Fig. 4a). MTT reduction was not affected by PLD1i. Subcellular ERK1/2 localization was also affected by PLD1 inhibition in ut cells. Whereas under control conditions (vehicle) ut cells displayed cytosolic ERK1/2 localization, PLD1 inhibition promoted ERK1/2 nuclear translocation (Fig. 4b). These results demonstrate that PLD1 regulates not only p-ERK1/2 levels but also their cytosolic localization in ut cells. As mentioned above, WT α-syn neurons displayed increased levels of ERK1/2 nuclear content accompanied by PLD1 downregulation when compared with controls. Consistently, ERK1/2 nuclear localization triggered by WT α-syn overexpression was potentiated in the presence of PLD1i (Fig 4c). These data suggest that α-syn not only inhibits PLD1 expression but also regulates ERK1/2 subcellular localization in a PLD1-dependent manner.

3.5. PLD1 and ERK1/2 inhibition by WT α-syn is associated with NFL expression

It has been reported that PLD isoforms are involved in the regulation of cytoskeleton [34]. Specifically, PLD1 interacts with filamentous actin and colocalizes with stress fiber-like structures [35,36]. Moreover, Frohman's laboratory demonstrated that PLD1 knockdown produces an overload of F-actin in the cellular surface [37]. However, there are no preceding reports on the role of PLD in the regulation of neurofilament network. To study the association between PLD and the neurofilament loss, we first analyzed the expression of NFL in the presence of both PLD1i and a specific pharmacological PLD2

inhibitor (PLD2i), CAY10594, in the absence of α-syn overexpression. We observed that NFL expression was decreased only when PLD1 was inhibited, whereas it was not affected by the inhibition of PLD2 in IMR-32 ut neurons (Fig. 5a). Our results confirm that the inhibition of PA production catalyzed by PLD1 activity is associated with NFL expression in IMR-32 ut cells.

In order to establish the effect of both inhibitors on PA generation, PEth was used as a marker of PLD activity. In ut cells, the total PA production measured as PEth generation (100% =1162±123dpm/mg protein) in the absence of PLD1i and PLD2i represented the sum of both PLD activities (Fig. 5b). In ut cells, PLD1 contribution to PA levels was 61%, whereas PLD2 contribution was 36%. In WT α-syn cells, total PEth formation was similar to that observed in ut cells, but PLD1 and PLD2 contribution was different, since that PLD1i diminished only 30% PEth production. These results suggest a higher contribution of PLD2 to PA levels in WT α-syn neurons (Fig. 5c). Moreover, PEth production was reduced to background levels when WT α-syn cells were treated with both inhibitors.

To evaluate the influence of the pharmacological PLD1 inhibition on the NFL loss induced by α-syn, we also treated WT α-syn neurons with PLD1i. Cells treated with PLD1i displayed a potentiated alteration of the NFL network, with almost complete abolishment of the protein expression. However, the neurofilament heavy subunit (NFH) expression levels were not affected neither by WT α-syn overexpression nor PLD1 inhibition (Fig. 6a).

To determine the role of PLD1 in the exaggerated F-actin polymerization observed in the cellular surface (Fig. 1d), we also incubated WT α-syn neurons with VU0155069. The presence of PLD1 inhibitor increased the foci of actin polymerization in the cellular periphery and in the sites of attachment to extracellular surroundings (Fig. 6b).

In order to establish whether the activity of ERK1/2 was associated with NFL expression, we used the pharmacological ERK1/2 inhibitor, U0126. The inhibition of ERK1/2 phosphorylation triggered a reduction in NFL expression in ut cells (Fig. 7a) and also slightly affected cell viability. NFL decrease was more evident in WT α-syn neurons incubated with the ERK1/2 inhibitor (Fig.7b).

3.6. Overexpression of PLD1 and ERK2 in WT α-syn neurons restores NFL expression

As our results suggest that PLD1 and ERK1/2 are associated with NFL expression, we hypothesized that restoration of PLD1 and ERK2 levels might either revert or prevent the loss of NFL. For this purpose, WT α-syn neurons were transiently transfected with wild-type PLD1 tagged with the green fluorescent protein (eGFP-PLD1). As transfection efficiency was less than 30%, WT α-syn neurons with negative green fluorescence were evaluated as the control condition. Neurons with positive green fluorescence showed increased levels of NFL (Fig. 8a). Furthermore, cells transiently transfected with eGFP-PLD2 or GFP empty vector showed no significant changes in NFL expression levels compared with non-transfected cells (Fig. 8b and c) These findings suggest that the recovery of PLD1 but not PLD2 expression restores NFL levels in WT α-syn neurons and strengthen the observation that the decrease in PLD1 levels triggered by α-syn overexpression could be responsible for NFL loss. Moreover, wild-type ERK2 was transiently expressed by using a HA-tagged vector (HA-ERK2). HA-positive WT α-syn neurons also showed increased NFL expression (Fig.8b). These observations reinforce the hypothesis that ERK1/2 downregulation and nuclear sequestration induced by α-syn are also related with NFL loss.

4. Discussion

Based on different biochemistry and cell biology approaches we have identified an inhibitory mechanism of PLD1 and ERK1/2 mediated by WT α-syn in human neuroblastoma cells. Furthermore, we observed that PLD1 and ERK1/2 inhibition were associated with a decrease in the expression of the neuronal marker NFL (Fig. 9). The increased expression of α-syn in IMR-32 neurons and the consequent PLD1 and NFL loss barely reduced cell viability (20%). Comparable results regarding cell viability were previously reported for the murine neuroblastoma N2A cell line expressing WT α-syn or its mutant A30P and for SH-SY5Y human neuroblastoma cells incubated with exogenous A53T α-syn mutant [31,38]. This could indicate that, in our experimental model, WT α-syn overexpression triggers mild neuronal injury related with the early stages of PD-associated neurodegeneration.

A number of genetic studies have contributed significantly to the understanding of α-syn gene (SNCA) and its involvement in PD [9,39]. On the basis of these studies, it is unquestionable that α-syn is one of the most important proteins involved in this pathology [9]. Therefore, it has been demonstrated that dramatic phenotypes can be triggered by slight alterations in α-syn overexpression [39]. Moreover, affected individuals, with 4 copies of SNCA, were found to have a corresponding doubling of SNCA mRNA and α-syn protein which was indeed sufficient to generate the Parkinsonian phenotype [40]. Here, we found 200 % increase in WT α-syn overexpression strongly reduces PLD1 mRNA levels and protein expression. Coincidently, brain tissues from patients with LB dementia, where α-syn overexpression and aggregation are hallmarks, presented reduced levels of PLD1 [16].

Previous reports have shown that α-syn significantly regulates the expression of several genes such as c-Jun N-terminal kinase, caveolin-1 and Bcl-2 family [41,42]. In line with this, several reports have demonstrated the presence of α-syn in the nucleus, its DNA

binding capacity and its ability to regulate gene transcription [43–45]. Taking into account all the above-mentioned, it can be speculated that PLD1 downregulation could be a consequence of the modulation of gene expression by α-syn.

Our observations also demonstrate that α-syn overexpression triggers NFL decrease. Neurofilaments are intermediate filaments found in neurons and consist of three subunits: NFH, medium (NFM) and NFL. NFL is the obligate subunit for neurofilament polymerization that renders mature filaments (homopolymers or heteropolymers with NFH and NFM [46]. Since neurofilaments participate in the growth of axons during development and in axon maintenance for electrical transmission, they are crucial players for proper neuronal function. Alterations in the neurofilament network constitute a common finding in neurodegenerative processes [47]. We found that the pharmacological inhibition of PLD1 activity in non-transfected IMR-32 neurons was accompanied by diminished levels of NFL. In addition, NFL levels were not modified by the inhibition of PLD2 activity. These results suggest that NFL expression in neurons is a mechanism mediated by PA produced exclusively by PLD1.

Substantia nigra samples from PD patients showed reduced levels of NFM and NFL [30]. In addition, levels of NFL in the cerebrospinal fluid have been proposed as markers of PD progression and other neurodegenerative diseases [48]. The diminished NFL expression found in WT α-syn neurons was even more pronounced in the presence of PLD1 inhibitor. Since α-syn inhibits PLD1 expression, these results demonstrate that the inhibition of the remaining phospholipase activity in WT α-syn neurons almost abolished NFL expression. Furthermore, the overexpression of constitutively active PLD1 restored NFL levels in WT α-syn cells. Moreover, PLD2 inhibition or transient overexpression (eGFP-PLD2) did not revert the effect of α-syn on NFL. Our results suggest that PLD1 downregulation induced by α-syn is associated with a degenerative-

like phenotype, constituting the first evidence of a link between PLD1 and NFL impairment in a cellular model of PD. In line with our findings, it has been shown that neurons from PLD1$^{-/-}$ mice showed altered dendritic branching and reduced secondary dendritic processes [5]. We also demonstrate here that PLD1 inhibition by α-syn is associated with cytoskeletal F-actin arrangement. These findings are in agreement with other reports on the biological implications of PLD1 and α-syn. One of these, published by the Frohman´s group, reports that PLD1 knockdown produces exaggerated F-actin polymerization in macrophages [37]. Another, from Chieregatti's laboratory, demonstrates that WT α-syn is able to bind actin and to slow down its polymerization rate [31]. Our results are in accordance with previous findings and show that actin cytoskeleton impairment is triggered by the diminished expression of PLD1; α-syn might therefore affect several cellular processes, thus contributing to the pathogenesis of PD.

In previous work from our laboratory we have shown that ERK1/2 activation during neuronal response to oxidative stress is dependent on PLD1 activity [18]. We also reported that inflammatory processes triggered by lipopolysaccharide involve ERK and protein kinase C activation, both regulated by PLD1 [19]. PLD1 modulation of MEK/ERK1/2 activity was also reported in rat lacrimal acini [49]. More recently, it has been demonstrated that PLD1 regulates the ERK1/2-CREB pathway in neuronal primary culture of cerebral cortex as part of the molecular machinery necessary for neuronal response to brain derived neurotrophic factor [50]. In our experimental set-up, we observed that under basal conditions ERK1/2 phosphorylation was also PLD1-dependent in IMR-32 ut neurons. We show here that PLD1 is predominantly located in the nucleus, in agreement with previous studies reporting that its nuclear localization mediates PKC and ERK cytosolic signaling [51]. We also demonstrate that both the

inhibition of PLD1 and the presence of α-syn promote an increase in ERK1/2 nuclear localization. It is possible that nuclear ERK1/2 localization induced by α-syn overexpression avoids its activation in the cytosol. In this connection, earlier work from Nukina's laboratory demonstrated that α-syn binding to MAPK occurs in neurons, thus promoting pathway inhibition [33,52]. We found that transiently transfected ERK2 promotes NFL recovery in WT α-syn neurons. In this regard, NFL phosphorylation in the tail domain is catalyzed by ERK1/2 kinases and this phosphorylation is crucial for conferring resistance to proteolysis [47,53]. In line with this, a natural compound derived from *Dioscorea* sp. promotes neurite outgrowth and increases NFL mRNA levels through ERK1/2 activation in PC12 cells [54]. Taking into account the above-mentioned evidence and our current findings, it can be hypothesized that ERK1/2 signaling is both directly and indirectly (via PLD1 inhibition) regulated by α-syn, finally impacting on NFL expression.

In the current study, we show that the overexpression of WT α-syn inhibits PLD1 expression and also affects ERK1/2 signaling in a phospholipase-dependent manner. Both PLD1 and ERK1/2 inhibition were associated with NFL loss in WT α-syn neurons. Our results confirm previous findings related to PLD1 downregulation by α-syn overexpression in *post mortem* brains and also provide new insights into the role of PLD1 in neuronal cell biology during parkinsonian neurodegeneration.

Acknowledgements

This work was supported by the Agencia Nacional de Promoción Científica y Tecnológica www.agencia.mincyt.gob.ar/ [PICT2010-0936, PICT2013-0987] to GAS; Consejo Nacional de Investigaciones Científicas y Técnicas www.conicet.gov.ar [PIP1122009010068] to GAS and the Universidad Nacional del Sur www.uns.edu.ar [PGI24B226] to GAS. The funders had no role in study design, data collection and

analysis, decision to publish, or preparation of the manuscript. Authors wish to thank Dr. B. Wolozin for kindly providing the WT α-syn DNA construct, Dr. M. Frohman and Dr. S. Gutking for kindly providing eGFP-PLD1/PLD2 and HA-ERK2 constructs, respectively, Dr. F. Villarreal, Dr. G. Mackenzie and Dr. A. Roccamo for their helpful assistance in molecular biology techniques and translator V. Soler for her assistance in English editing.

Conflict of interests

The author(s) declare no conflict of interests.

References

[1] H.A. Brown, P.G. Thomas, C.W. Lindsley, Targeting phospholipase D in cancer, infection and neurodegenerative disorders, Nat. Rev. Drug Discov. 16 (2017) 351–367. doi:10.1038/nrd.2016.252.

[2] Y. Liu, Y. Su, X. Wang, Phosphatidic acid-mediated signaling, Adv. Exp. Med. Biol. 991 (2013) 159–176. doi:10.1007/978-94-007-6331-9-9.

[3] X. Wang, S.P. Devaiah, W. Zhang, R. Welti, Signaling functions of phosphatidic acid, Prog. Lipid Res. 45 (2006) 250–278. doi:10.1016/j.plipres.2006.01.005.

[4] X. Peng, M.A. Frohman, Mammalian phospholipase D physiological and pathological roles, Acta Physiol. 204 (2012) 219–226. doi:10.1111/j.1748-1716.2011.02298.x.

[5] M.R. Ammar, Y. Humeau, A. Hanauer, B. Nieswandt, M.F. Bader, N. Vitale, The Coffin-Lowry Syndrome-Associated Protein RSK2 Regulates Neurite Outgrowth through Phosphorylation of Phospholipase D1 (PLD1) and Synthesis of Phosphatidic Acid, J. Neurosci. 33 (2013) 19470–19479. doi:10.1523/JNEUROSCI.2283-13.2013.

[6] M.R. Ammar, N. Kassas, M.F. Bader, N. Vitale, Phosphatidic acid in neuronal

development: A node for membrane and cytoskeleton rearrangements, Biochimie. (2014) 51–57. doi:10.1016/j.biochi.2014.07.026.

[7] D.M. Raben, C.N. Barber, Phosphatidic acid and neurotransmission, Adv. Biol. Regul. 63 (2017) 15–21. doi:10.1016/j.jbior.2016.09.004.

[8] C.M. Tolleson, J.Y. Fang, Advances in the mechanisms of Parkinson's disease, Discov. Med. 15 (2013) 61–66.

[9] J. Hardy, Genetic analysis of pathways to Parkinson disease, Neuron. 68 (2010) 201–206. doi:10.1016/j.neuron.2010.10.014.

[10] V. Ruipérez, F. Darios, B. Davletov, Alpha-synuclein, lipids and Parkinson's disease, Prog. Lipid Res. 49 (2010) 420–428. doi:10.1016/j.plipres.2010.05.004.

[11] M.Y. Golovko, G. Barceló-Coblijn, P.I. Castagnet, S. Austin, C.K. Combs, E.J. Murphy, The role of α-synuclein in brain lipid metabolism: A downstream impact on brain inflammatory response, Mol. Cell. Biochem., 2009: pp. 55–66. doi:10.1007/s11010-008-0008-y.

[12] M.Y. Golovko, T.A. Rosenberger, S. Feddersen, N.J. Færgeman, E.J. Murphy, α-Synuclein gene ablation increases docosahexaenoic acid incorporation and turnover in brain phospholipids, J. Neurochem. 101 (2007) 201–211. doi:10.1111/j.1471-4159.2006.04357.x.

[13] R. Sharon, I. Bar-Joseph, G.E. Mirick, C.N. Serhan, D.J. Selkoe, Altered fatty acid composition of dopaminergic neurons expressing alpha-synuclein and human brains with alpha-synucleinopathies, J. Biol. Chem. 278 (2003) 49874–49881. doi:10.1074/jbc.M309127200M309127200 [pii].

[14] O.S. Gorbatyuk, S. Li, F.N. Nguyen, F.P. Manfredsson, G. Kondrikova, L.F. Sullivan, C. Meyers, W. Chen, R.J. Mandel, N. Muzyczka, α-Synuclein expression in rat substantia nigra suppresses phospholipase D2 toxicity and nigral

neurodegeneration, Mol. Ther. 18 (2010) 1758–68. doi:10.1038/mt.2010.137.

[15] I. Rappley, A.D. Gitler, P.E. Selvy, M.J. LaVoie, B.D. Levy, H.A. Brown, S. Lindquist, D.J. Selkoe, Evidence that alpha-synuclein does not inhibit phospholipase D, Biochemistry. 48 (2009) 1077–1083. doi:10.1021/bi801871h.Evidence.

[16] E.J. Bae, H.J. Lee, Y.H. Jang, S. Michael, E. Masliah, D.S. Min, S.J. Lee, Phospholipase D1 regulates autophagic flux and clearance of α-synuclein aggregates, Cell Death Differ. 21 (2014) 1132–1141. doi:10.1038/cdd.2014.30.

[17] M.V. Mateos, R.M. Uranga, G.A. Salvador, N.M. Giusto, Activation of phosphatidylcholine signalling during oxidative stress in synaptic endings, Neurochem. Int. 53 (2008) 199–206. doi:10.1016/j.neuint.2008.07.005.

[18] M.V. Mateos, N.M. Giusto, G.A. Salvador, Distinctive roles of PLD signaling elicited by oxidative stress in synaptic endings from adult and aged rats, Biochim. Biophys. Acta - Mol. Cell Res. 1823 (2012) 2136–2148. doi:10.1016/j.bbamcr.2012.09.005.

[19] M.V. Mateos, C.B. Kamerbeek, N.M. Giusto, G.A. Salvador, The phospholipase D pathway mediates the inflammatory response of the retinal pigment epithelium, Int. J. Biochem. Cell Biol. 55 (2014). doi:10.1016/j.biocel.2014.08.016.

[20] U. Burkhardt, D. Stegner, E. Hattingen, S. Beyer, B. Nieswandt, J. Klein, Impaired brain development and reduced cognitive function in phospholipase D-deficient mice, Neurosci. Lett. 572 (2014) 48–52. doi:10.1016/j.neulet.2014.04.052.

[21] M.A. Frohman, The phospholipase D superfamily as therapeutic targets, Trends Pharmacol. Sci. 36 (2015) 137–144. doi:10.1016/j.tips.2015.01.001.

[22] S.S. Campos, G.R. Diez, G.M. Oresti, G.A. Salvador, Dopaminergic neurons

respond to iron-induced oxidative stress by modulating lipid acylation and deacylation cycles, PLoS One. 10 (2015). doi:10.1371/journal.pone.0130726.

[23] M.M. Bradford, A rapid and sensitive method for the quantitation of microgram quantities of protein utilizing the principle of protein-dye binding, Anal. Biochem. 72 (1976) 248–254. doi:10.1016/0003-2697(76)90527-3.

[24] U.K. Laemmli, Cleavage of Structural Proteins during the Assembly of the Head of Bacteriophage T4, Nature. 227 (1970) 680–685. doi:10.1038/227680a0.

[25] C. Arndt, S. Koristka, H. Bartsch, M. Bachmann, Native polyacrylamide gels, Methods Mol. Biol. 869 (2012) 49–53. doi:10.1007/978-1-61779-821-4_5.

[26] R.M. Uranga, S. Katz, G.A. Salvador, Enhanced phosphatidylinositol 3-kinase (PI3K)/Akt signaling has pleiotropic targets in hippocampal neurons exposed to iron-induced oxidative stress, J. Biol. Chem. 288 (2013) 19773–19784. doi:10.1074/jbc.M113.457622.

[27] G.A. Salvador, N.M. Giusto, Characterization of phospholipase D activity in bovine photoreceptor membranes, Lipids. 33 (1998) 853–860. doi:10.1007/s11745-998-0281-z.

[28] M.V. Mateos, G.A. Salvador, N.M. Giusto, Selective localization of phosphatidylcholine-derived signaling in detergent-resistant membranes from synaptic endings, Biochim. Biophys. Acta - Biomembr. 1798 (2010) 624–636. doi:10.1016/j.bbamem.2009.12.008.

[29] G. Rouser, S. Fleischer, A. Yamamoto, Two dimensional thin layer chromatographic separation of polar lipids and determination of phospholipids by phosphorus analysis of spots, Lipids. 5 (1970) 494–496. doi:10.1007/BF02531316.

[30] M. Basso, S. Giraudo, D. Corpillo, B. Bergamasco, L. Lopiano, M. Fasano,

Proteome analysis of human substantia nigra in Parkinson's disease, Proteomics. 4 (2004) 3943–3952. doi:10.1002/pmic.200400848.

[31] V.L. Sousa, S. Bellani, M. Giannandrea, M. Yousuf, F. Valtorta, J. Meldolesi, E. Chieregatti, α-Synuclein and Its A30P Mutant Affect Actin Cytoskeletal Structure and Dynamics, Mol. Biol. Cell. 20 (2009) 3725–3739. doi:10.1091/mbc.E08-03-0302.

[32] J.E. Payton, R.J. Perrin, W.S. Woods, J.M. George, Structural determinants of PLD2 inhibition by α-synuclein, J. Mol. Biol. 337 (2004) 1001–1009. doi:10.1016/j.jmb.2004.02.014.

[33] A. Iwata, M. Maruyama, I. Kanazawa, N. Nukina, α-Synuclein Affects the MAPK Pathway and Accelerates Cell Death, J. Biol. Chem. 276 (2001) 45320–45329. doi:10.1074/jbc.M103736200.

[34] S.A. Rudge, M.J.O. Wakelam, Inter-regulatory dynamics of phospholipase D and the actin cytoskeleton, Biochim. Biophys. Acta - Mol. Cell Biol. Lipids. 1791 (2009) 856–861. doi:10.1016/j.bbalip.2009.04.008.

[35] M.J. Farquhar, D.J. Powner, B.A. Levine, M.H. Wright, G. Ladds, M.N. Hodgkin, Interaction of PLD1b with actin in antigen-stimulated mast cells, Cell. Signal. 19 (2007) 349–358. doi:10.1016/j.cellsig.2006.07.016.

[36] H. Komati, F. Naro, S. Mebarek, V. De Arcangelis, S. Adamo, M. Lagarde, A.-F. Prigent, G. Nemoz, Phospholipase D is involved in myogenic differentiation through remodeling of actin cytoskeleton, Mol. Biol. Cell. 16 (2005) 1232–1244. doi:E04-06-0459 [pii]\r10.1091/mbc.E04-06-0459.

[37] W.H. Ali, Q. Chen, K.E. Delgiorno, W. Su, J.C. Hall, T. Hongu, H. Tian, Y. Kanaho, G. Di Paolo, H.C. Crawford, M.A. Frohman, Deficiencies of the Lipid-Signaling Enzymes Phospholipase D1 and D2 Alter Cytoskeletal Organization,

Macrophage Phagocytosis, and Cytokine-Stimulated Neutrophil Recruitment, PLoS One. 8 (2013). doi:10.1371/journal.pone.0055325.

[38] T. Okada, C. Hirai, S.M.M. Badawy, L. Zhang, T. Kajimoto, S. Nakamura, Impairment of PDGF-induced chemotaxis by extracellular α-synuclein through selective inhibition of Rac1 activation, Sci. Rep. 6 (2016) 37810. doi:10.1038/srep37810.

[39] M.J. Devine, K. Gwinn, A. Singleton, J. Hardy, Parkinson's disease and α-synuclein expression, Mov. Disord. 26 (2011) 2160–2168. doi:10.1002/mds.23948.

[40] D.W. Miller, S.M. Hague, J. Clarimon, M. Baptista, K. Gwinn-Hardy, M.R. Cookson, A.B. Singleton, Alpha-synuclein in blood and brain from familial Parkinson disease with SNCA locus triplication, Neurology. 62 (2004) 1835–1838. doi:10.1212/01.WNL.0000127517.33208.F4.

[41] M. Hashimoto, T. Takenouchi, E. Rockenstein, E. Masliah, α-synuclein up-regulates expression of caveolin-1 and down-regulates extracellular signal-regulated kinase activity in B103 neuroblastoma cells: Role in the pathogenesis of Parkinson's disease, J. Neurochem. 85 (2003) 1468–1479. doi:10.1046/j.1471-4159.2003.01791.x.

[42] J.H. Seo, J.C. Rah, S.H. Choi, J.K. Shin, K. Min, H.S. Kim, C.H. Park, S. Kim, E.M. Kim, S.H. Lee, S. Lee, S.W. Suh, Y.H. Suh, Alpha-synuclein regulates neuronal survival via Bcl-2 family expression and PI3/Akt kinase pathway, FASEB J. 16 (2002) 1826–1828. doi:10.1096/fj.02-0041fje.

[43] M.J. Baptista, C. O'Farrell, S. Daya, R. Ahmad, D.W. Miller, J. Hardy, M.J. Farrer, M.R. Cookson, Co-ordinate transcriptional regulation of dopamine synthesis genes by alpha-synuclein in human neuroblastoma cell lines, J.

Neurochem. 85 (2003) 957–968. doi:10.1046/j.1471-4159.2003.01742.x.

[44] K.L. Ma, L.K. Song, Y.H. Yuan, Y. Zhang, J.L. Yang, P. Zhu, N.H. Chen, α-synuclein is prone to interaction with the GC-box-like sequence in vitro, Cell. Mol. Neurobiol. 34 (2014) 603–609. doi:10.1007/s10571-014-0046-9.

[45] A.A. Surguchev, A. Surguchov, Synucleins and Gene Expression: Ramblers in a Crowd or Cops Regulating Traffic?, Front. Mol. Neurosci. 10 (2017). doi:10.3389/fnmol.2017.00224.

[46] M.K. Lee, Z. Xu, P.C. Wong, D.W. Cleveland, Neurofilaments are obligate heteropolymers in vivo, J. Cell Biol. 122 (1993) 1337–1350. doi:10.1083/jcb.122.6.1337.

[47] A. Yuan, M.V. Rao, Veeranna, R.A. Nixon, Neurofilaments at a glance, J. Cell Sci. 125 (2012) 3257–3263. doi:10.1242/jcs.104729.

[48] O. Hansson, S. Janelidze, S. Hall, N. Magdalinou, A.J. Lees, U. Andreasson, N. Norgren, J. Linder, L. Forsgren, R. Constantinescu, H. Zetterberg, K. Blennow, Blood-based NfL: A biomarker for differential diagnosis of parkinsonian disorder, Neurology. 88 (2017) 930–937. doi:10.1212/WNL.0000000000003680.

[49] R.R. Hodges, E. Guilbert, M.A. Shatos, V. Natarajan, D.A. Dartt, Phospholipase D1, but not D2, Regulates protein secretion Via Rho/ROCK in a Ras/Raf-independent, MEK-dependent manner in rat lacrimal gland, Investig. Ophthalmol. Vis. Sci. 52 (2011) 2199–2210. doi:10.1167/iovs.10-6209.

[50] M.R. Ammar, T. Thahouly, A. Hanauer, D. Stegner, B. Nieswandt, N. Vitale, PLD1 participates in BDNF-induced signalling in cortical neurons, Sci. Rep. 5 (2015) 14778. doi:10.1038/srep14778.

[51] Y.H. Jang, D.S. Min, Nuclear localization of phospholipase D1 mediates the activation of nuclear protein kinase C(alpha) and extracellular signal-regulated

kinase signaling pathways, J. Biol. Chem. 286 (2011) 4680–4689. doi:10.1074/jbc.M110.162602.

[52] A. Iwata, S. Miura, I. Kanazawa, M. Sawada, N. Nukina, alpha-Synuclein forms a complex with transcription factor Elk-1, J. Neurochem. 77 (2001) 239–52. doi:10.1046/j.1471-4159.2001.00232.x.

[53] H.C. Pant, Dephosphorylation of neurofilament proteins enhances their susceptibility to degradation by calpain, Biochem. J. 256 (1988) 665–668. doi:10.1042/bj2560665.

[54] J.H. Won, K.H. Ahn, M.J. Back, H.C. Ha, J.M. Jang, H.H. Kim, S. Choi, M. Son, D.K. Kim, DA-9801 promotes neurite outgrowth via ERK1/2-CREB pathway in PC12 cells, Biol. Pharm. Bull. 38 (2015) 169–78. doi:10.1248/bpb.b14-00236.

Figure legends

Fig. 1. Characterization of the neuronal model of α-syn overexpression. a, representative immunoblots of α-syn expression levels in lysates from IMR-32 cells transfected with the empty pcDNA vector (ev) or with the plasmid expressing human wild type α-syn (α-syn). Non-denaturing gels show the cellular levels of α-syn monomers and oligomers. One representative blot of three different experiments is presented. Bands of α-syn monomer (19 kDa) of the SDS-PAGE were quantified through scanning densitometry. The data in the graph on the right represent the ratio between α-syn monomer and β-actin (mean ± SD of three different experiments, $^{**}p < 0.01$ with respect to the control). b, immunocytochemistry studies were performed using antibodies against neurofilament light subunit (NFL) to evaluate its expression in IMR-32 neurons after transfections. Hoechst was used as nuclear marker. Images of at least three different experiments are presented. Fluorescence intensity quantification

(arbitrary units, AU) is shown in the graph on the right (***p< 0.001 with respect to the corresponding control conditions). c, microscopic visualization of F-actin arrangement through fluorescent phalloidin in the neuronal model of α-syn overexpression. Arrows indicate the actin-enriched loci in the cellular surface displayed by the α-syn cells. Nuclei were stained with Hoechst. Images represent at least three different experiments. Fluorescence intensity quantification is shown on the right (ns= no significant difference with respect to the corresponding control condition). d, cell viability was measured by the MTT reduction assay. Results are expressed as AU and represent mean ± SD (n= 8-14). ***p< 0.001with respect to the control.

Fig. 2. Influence of α-syn on PLD1 expression. a, Western blots showing the expression levels of PLD1 in ev and α-syn neurons from two independent experiments. Both blots derive from the same experiments and were processed in parallel. The 100 kDa molecular weight marker is shown. The blots shown are representative of four different experiments. Bands of proteins were quantified by scanning densitometry. The ratio between PLD1 and β-actin is represented in the graph on the right as a percentage of the control condition (mean ± SD***p< 0.001 with respect to the corresponding control). b, qRT-PCR analysis for PLD1 transcripts in ev and α-syn cells. Data were normalized to RiboL32 as internal reference gen using the $2^{-\Delta Ct}$ method (mean ± SD of three different experiments, ***p< 0.001 with respect to the control). c, IMR-32 ut, ev and α-syn cells were grown on coverslips and after fixation immunostained with anti-PLD1 antibody. Nuclei were marked with Hoechst. Images are representative of at least three different experiments. The data in the graphs on the right represent AU of fluorescence intensity (mean ± SD of three different experiments, ***p< 0.001 with respect to the control).

Fig. 3. Effect of WT α-syn on ERK1/2 status. a, phosphorylation of ERK1/2 and their cellular levels were evaluated through Western blot of lysates from neurons expressing α-syn and controls (ev). Both blots derive from the same experiment and were processed in parallel. The blots shown are representative of three different experiments. The data in the graph on the right represent the ratio between protein phosphorylation or expression levels and α-tubulin (percentage of the corresponding control condition; mean ± SD of three different experiments); *$p< 0.05$ and **$p< 0.01$ with respect to the control. b, ERK2 expression and subcellular distribution were also investigated by immunocytochemistry using anti-ERK2 antibody to stain ut, ev and α-syn cells. Hoechst was used as nuclear marker. Images are representative of at least three different experiments. Quantification results of the fluorescence intensity (AU) are presented in the graph on the right panel. ***$p< 0.001$ with respect to the control. c, to determine ERK1/2 level in nuclear and cytosolic fractions of ev and α-syn cells, Western blot analysis was performed. hnRNP was used as nuclear marker and α-tubulin was used as cytosolic marker. Bands of proteins were quantified using scanning densitometry in cytosolic (CF) and nuclear (NF) fractions. The data in the graph on the right represent the ratio between nuclear ERK1/2/hnRNP and cytosolic ERK1/2/α-tubulin of three different experiments. *$p< 0.05$ for each condition with respect to the control.

Fig. 4. Modulation of PLD1/ERK1/2 signaling by WT α-syn. The effect of PLD1 on ERK1/2 activation and expression was evaluated in neurons treated with VU0155069 (pharmacological PLD1 inhibitor, PLD1i) or its vehicle. a, Western blot showing ERK1/2 phosphorylation and total levels in ut neurons incubated with PLD1i. Both blots derive from the same experiment and were processed in parallel. Representative blots of three different experiments are shown. The data in the graph on the middle

panel represent the ratio between p-ERK1/2 and ERK1/2 (percentage of the control condition; mean ± SD of three different experiments). Scanning densitometry was used for band quantification; *p< 0.05 with respect to the control. MTT reduction assay in ut cells in the presence of PLD1i is shown on the right panel (results are expressed as a percentage of the control condition). b, ERK1/2 nuclear translocation induced by PLD1i was analyzed by immunocytochemistry in ut cells. The data in the right-hand graph represent fluorescence intensity in AU (mean ± SD of three different experiments, ***p< 0.001 with respect to the control). c, immunocytochemistry studies using anti-ERK1/2 antibody under PLD1i conditions in cells overexpressing α-syn. b and c, Hoechst was used as nuclear marker. Images of at least three different experiments are presented. The data in the graphs on the right represent the ERK1/2 fluorescence intensity (mean ± SD of three different experiments, ***p< 0.001 with respect to the control).

Fig. 5. PLD1 activity is related to NFL loss. a, immunocytochemistry with anti-NFL antibody in PLD1i- and PLD2i-treated ut neurons. Nuclei were marked with Hoechst. Representative images of at least three different experiments are shown. Quantification results of the fluorescence intensity (AU) are presented in the graph on the right panel. ***p< 0.001 with respect to the control. b, PLD activity was measured as [^{3}H]-PEth formation in ut cells incubated with PLD1i and PLD2i. Results are expressed as percentage of the control condition (mean value ± SD of three independent experiments; *p< 0.05 and **p< 0.01 with respect to the control). c, PLD activity was evaluated in α-syn cells in the presence of PLD1i, PLD2i and both inhibitors. Results are expressed as percentage of the control conditions (mean value ± SD of three independent experiments; *p< 0.05 and ***p< 0.001 with respect to the control).

Fig. 6. NFL expression is regulated by PLD1 in α-syn neurons. The role of PLD1 in the modulation of NLF levels was studied in the presence of PLD1i (VU0155069) or its vehicle. a, after treatments, NFL expression was determined by immunocytochemistry in ev and α-syn cells. Hoechst was used as nuclear marker. Images are representative of at least three different experiments. Representative images of NFL and NFH expression in Western blot studies are shown on the right (top). The data in the graph on the right represent NFL fluorescence intensity (down) (mean ± SD of three different experiments, $*p< 0.05$ and $***p< 0.001$ with respect to the control). b, microscopic analysis of VU0155069-treated cells labeled with phalloidin. Arrows show the peripheral foci of actin polymerization. Representative images of at least three experiments are presented. Quantification results of the F-actin fluorescence intensity (AU) are shown in the graph on the right panel (ns= no significant difference with respect to the control).

Fig. 7. ERK1/2 modulate NFL expression in ut and α-syn neurons. To investigate whether NFL levels are influenced by ERK1/2 activity, cells were incubated with U0126 (MEK1/2 inhibitor) or its vehicle. a, immunocytochemistry showing NFL expression levels under ERK1/2 inhibition in ut cells (left panel). NFL fluorescence intensity quantification is shown on the middle panel; results are presented as arbitrary units. The MTT reduction assay in ut cells treated with U0126 is also shown on the right panel; results are presented as a percentage of the control, $*p< 0.05$ with respect to the control. b, immunocytochemistry studies showing NFL expression in α-syn and ev neurons after incubation with ERK1/2 inhibitor. a and b, nuclei were marked with Hoechst. Representative images of at least three different independent experiments are

shown. The data in the graphs on the right represent fluorescence intensity (mean ± SD of three different experiments, $^{**}p < 0.01$ and $^{***}p < 0.001$ with respect to the control).

Fig. 8. Reestablishment of NFL levels by overexpression of PLD1 and ERK2. α-syn neurons were transfected with eGFP-hPLD1b, eGFP-hPLD2, GFP empty vector or HA-ERK2 and cultured for 48 h. Cells were then processed for immunocytochemistry studies with antibodies against NFL (a-d). Nuclei were stained with TO-PRO®-3 (a-c) or Hoechst (d). Transfected as well as non-transfected (eGFP-PLD1-negative, eGFP-PLD2-negative, GFP-negative or HA-ERK2-negative) cells (used as control conditions) are shown in the same field. Representative images of at least three different independent experiments are shown. The data in the graphs on the right represent fluorescence intensity (AU- mean ± SD of three different experiments, $^{***}p < 0.001$ with respect to the control).

Fig. 9. Representative scheme shows the effects of PLD1 inhibition triggered by α-syn overexpression and the potential implications in neuronal degeneration.

Highlights

We studied the impact of WT α-syn overexpression on PLD1 signaling.

Overexpression of WT α-syn downregulates PLD1 and NFL expression.

ERK1/2 is downregulated and mainly located in nuclear fraction in WT α-syn neurons.

Pharmacological PLD1 inhibition triggers NFL loss and ERK1/2 nuclear localization in non-transfected neurons.

Overexpression of eGFP-PLD1 reestablishes NFL levels in WT α-syn neurons.